Hyperbolic Metamaterials with Bragg Polaritons

Evgeny S. Sedov,[1,2,*] I. V. Iorsh,[2] S. M. Arakelian,[1] A. P. Alodjants,[1,2,3,†] and Alexey Kavokin[3,4,5]
[1]Department of Physics and Applied Mathematics, Vladimir State University named after A. G. and N. G. Stoletovs, Gorky street 87, 600000 Vladimir, Russia
[2]National Research University for Information Technology, Mechanics and Optics (ITMO), St. Petersburg 197101, Russia
[3]Russian Quantum Center, Novaya 100, 143025 Skolkovo, Moscow Region, Russia
[4]Spin Optics Laboratory, St. Petersburg State University, Ul'anovskaya, Peterhof, St. Petersburg 198504, Russia
[5]School of Physics and Astronomy, University of Southampton, SO17 1BJ Southampton, United Kingdom
(Received 8 September 2014; published 10 June 2015)

We propose a novel mechanism for designing quantum hyperbolic metamaterials with the use of semiconductor Bragg mirrors containing periodically arranged quantum wells. The hyperbolic dispersion of exciton-polariton modes is realized near the top of the first allowed photonic miniband in such a structure which leads to the formation of exciton-polariton X waves. Exciton-light coupling provides a resonant nonlinearity which leads to nontrivial topologic solutions. We predict the formation of low amplitude spatially localized oscillatory structures: oscillons described by kink shaped solutions of the effective Ginzburg-Landau-Higgs equation. The oscillons have direct analogies in gravitational theory. We discuss implementation of exciton-polariton Higgs fields for the Schrödinger cat state generation.

DOI: 10.1103/PhysRevLett.114.237402 PACS numbers: 78.67.Pt, 98.80.Cq

Introduction.—A remarkable similarity between propagation of electromagnetic waves in inhomogeneous media described by Maxwell's equations and propagation of photons in curved space-time described by the general relativity laws offers a possibility of designing media where light propagates along predefined curved trajectories. This concept, known as *transformation optics* [1] not only allowed emulating many gravitational effects such as gravitational lensing [2], event horizon [3], etc., but also led to a bunch of intriguing practical applications, such as optical cloaking [4], and superresolution optical imaging [5]. Construction of the media with predefined profiles of electric and magnetic permeabilities is feasible with use of *metamaterials* [6], artificial periodic structures whose optical properties are governed both by the electromagnetic response of individual structure elements and by the geometry of the lattice. Hyperbolic metamatrials (HMMs) are highly anisotropic media that have hyperbolic (or indefinite) dispersion [7], determined by their effective electric and/or magnetic tensors. Such structures represent the ultra-anisotropic limit of traditional uniaxial crystals. One of the diagonal components of either permittivity (ε) or permeability (μ) tensors of HMMs has an opposite sign with respect to the other two diagonal components. Recently, HMMs have attracted enhanced attention both due to the promising applications in quantum lifetime engineering [8] and subwavelength image transfer [9], and because of their relatively low production costs as compared to other optical metamaterial designs. In contrast to all-dielectric uniaxial anisotropic media for which both dielectric permittivities are positive: $\varepsilon_1 \equiv \varepsilon_x = \varepsilon_y > 0$ and $\varepsilon_2 \equiv \varepsilon_z > 0$, in HMMs ε_1 and ε_2 have opposite signs in some frequency ranges due to the presence of metallic layers. As a result, the analogy between wave propagation governed by the Helmholtz equation and the effective Klein-Gordon equation for a massive particle with a fictitious time coordinate can be obtained for the description of a coherent cw laser beam propagation in such a structure. This analogy makes possible the creation of the Minkowski space-time using HMMs [10]. Applications of HMMs for modeling gravity and cosmology problems within scalar ϕ^4-field theories require introducing a strong Kerr-like nonlinearity to the medium, [11,12]. However, the nonlinear response of the conventional HMMs is relatively weak. Moreover, most of the studied HMMs are essentially periodic arrays of metallic inclusions, characterised by large Ohmic losses and decay of the electromagnetic field propagation.

To overcome these problems, in this Letter we propose an approach for emulating quantum effects in curved space-time using exciton polaritons in multilayer semiconductor structures. Resonant HMMs may be realized in Bragg arranged semiconductor quantum wells (QWs) or other resonant photonic crystals [13]. We take advantage of the giant optical nonlinearity introduced due to the exciton-light coupling (cf. [14]) which is responsible for a number of nontrivial topology effects in coherent exciton-polariton fluids [15,16]. Specifically, in this Letter we consider resonant semiconductor Bragg mirrors as a model system for studying Higgs field properties. Light propagation in such structures has been extensively studied both theoretically and experimentally [17–22]. In particular, the dramatic modulation of the reflectivity spectra of Bragg spectra in the vicinity of exciton resonances was predicted

in Ref. [18]. The peculiar dispersion of mixed photon-exciton modes in Bragg arranged QWs has been discussed in the literature (see, e.g., Refs. [19–22]). Here we show that planar periodic semiconductor Bragg mirror structures with embedded QWs allow for controlling the signs of effective masses of mixed light-matter quasiparticles termed *Bragg exciton polaritons* in order to create a quantum HMM. The optical response of such a HMM can be tailored by tuning the layer thicknesses in a periodic structure [20].

Bragg mirror model.—The structure we consider is schematically shown in Fig. 1(a). It consists of the periodic array of alternating dielectric layers with QWs placed in the centers of the layers of one type. The exciton frequency is tuned to the high frequency edge of the second photonic band gap, which is characterized by the saddle point in the dispersion surface [20]. The Hamiltonian of the structure in Fig. 1(a) has a form $\hat{H} = \hat{H}_{\rm ph} + \hat{H}_X + \hat{H}_{\rm coup} + \hat{H}_{\rm nl}$ where $\hat{H}_{\rm ph}$ is the photonic part, $\hat{H}_X$ is the excitonic part, $\hat{H}_{\rm coup}$ accounts for the exciton-photon coupling, and $\hat{H}_{\rm nl}$ is the nonlinear part, which originated from the exciton-exciton scattering. In the vicinity of the second photonic band gap of the Bragg mirror one can diagonalize the linear part of the Hamiltonian $\hat{H}$, using the approach described in Ref. [19] to obtain the dispersions of four exciton-polariton branches $\mathcal{P}_1, \mathcal{P}_2, \mathcal{P}_3, \mathcal{P}_4$, which are shown in Fig. 1(b), see the Supplemental Material for more details [23]. Hereafter, we restrict ourselves only to the lower branch (LB) neglecting the inter-branch scattering processes.

To describe the LB polariton wave function (WF) associated with the Bragg mirror structure we start with the Gross-Pitaevskii equation (GPE) for a mean-field amplitude $\Psi(\mathbf{r}, t)$ [23]

$$i\hbar\frac{\partial\Psi}{\partial t} = \left[-\frac{\hbar^2}{2m_\parallel}\Delta_\parallel - \frac{\hbar^2}{2m_\perp}\frac{\partial^2}{\partial z^2} - i\hbar\gamma_0 + g|\Psi|^2\right]\Psi, \quad (1)$$

where $m_\parallel$ and $m_\perp$ are the components of the effective mass tensor. The nonlinear coupling constant can be approximated by $g \approx 6E_b a_b^3 D X_1^4/d_{\rm QW}$, where E_b is the exciton binding energy, a_b is the exciton Bohr radius, D is the period of the structure, $d_{\rm QW}$ is the QW width, and $V = L_x L_y L_z$ is the volume of the structure in Fig. 1, $X_1 \equiv X_1(0) \simeq 1/\sqrt{2}$ is the Hopfields coefficient for the lowest polariton branch; in Eq. (1) we neglect the nonlocal character of polariton-polariton interaction. We have introduced the dissipation term $-i\hbar\gamma_0$ to account for the radiative decay of polaritons. Here we consider a time-resolved response of the dissipative polariton system to the pulsed excitation which is accounted for in the initial condition. An important peculiarity of our system is the negative transverse component of the polaritonic effective mass that tends to $m_\perp = -2\pi^2\hbar\Omega_B(n_1+n_2)^2/n_1 n_2 D^2\omega_B(\omega_B - \Omega_B)$, where ω_B is the center of the second photonic band gap, Ω_B is the band gap half-width, $n_{1,2}$ are refractive indices of the layers. Meanwhile, the lateral effective mass $m_\parallel = 2\hbar n_1^2 n_2^2(\omega_B - \Omega_B)/c^2(n_1^2 - n_1 n_2 + n_2^2)$ is positive.

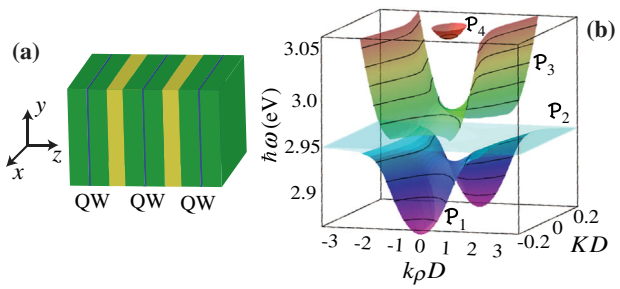

FIG. 1 (color online). (a) Schematic picture of the spatially periodical structure ("Bragg mirror"). (b) Dispersion surface for the $GaN/Al_{0.3}Ga_{0.7}N$ Bragg mirror with $In_{0.12}Ga_{0.88}N$ QWs placed in the centers of the GaN layers. The parameters of the system are given in the text.

Notably the LB of polaritons is characterized by the effective mass tensor whose diagonal components differ in sign. In general the effective mass tensor is dispersive due to the nonparabolicity of the polariton band; however, for the wave vectors that are small compared to the inverse period of the structure $1/D$, one can safely assume the tensor components are constant. Note that due to the smallness of the effective mass, exciton polaritons remain within the light cone, i. e., at the wave vectors smaller than $1/D$, even at room temperature.

In the numerical calculations, we consider a GaN/AlGaN layered structure with narrow InGaN QWs, for which the exciton binding energy E_b is approximately 45 meV, the exciton Bohr radius is $a_b \approx 18$ nm, $d_{\rm QW} = 10$ nm, and Rabi frequency $\Omega_P \approx 2\pi \times 7.1$ THz. Thicknesses of the layers and their refractive indices are taken as $d_1 = 64.8$ nm, $n_1 = 2.55$ and $d_2 = 115.3$ nm, $n_2 = 2.15$, period of the lattice $D = d_1 + d_2$ is 180.1 nm; ω_B is calculated as approximately $2\pi \times 726.2$ THz and the photonic band gap width Ω_B is about $2\pi \times 12.1$ THz. The polariton decay rate γ_0 is given by the photonic radiative decay lifetime $\tau = 1/\gamma_0$.

We transform Eq. (1) to the standard GPE by introducing the new variable $\Psi(\mathbf{r}, t) = \phi(\mathbf{r}, t)e^{-\gamma_0 t}$ as

$$i\hbar\partial_t\phi = \left[-\frac{\hbar^2}{2m_\parallel}\Delta_\parallel + \frac{\hbar^2}{2m}\partial_{zz} + p(t)^{-1}g|\phi|^2\right]\phi, \quad (2)$$

where we denote $m \equiv |m_\perp|$. In Eq. (2) we suppose that $e^{-2\gamma_0 t} \approx 1 - 2\gamma_0 t \equiv p(t)^{-1}$, cf. Ref. [26]. This approach is applicable in the limit of $\gamma_0 \ll \Omega_P$, or at the time scale such as $t < 1/\gamma_0$. We focus on the stationary states of LB polaritons representing the solution of Eq. (2) in the form

$$\varphi(X,Y,Z)=\sqrt{\frac{\kappa^2\kappa_z}{p(t)^3}}\phi(\mathbf{r},t)\times\exp\left[i\frac{\gamma_0 m_\parallel p(t)}{\hbar}\left(x^2+y^2-\frac{m}{m_\parallel}z^2\right)+i\frac{E}{\hbar}p(t)t\right], \tag{3}$$

where $\kappa=\hbar\sqrt{V/2m_\parallel g}$, $\kappa_z=\hbar\sqrt{V/2mg}$ are characteristic macroscopic scales of the polaritonic system in the structure, E is the energy of the system. Substituting Eq. (3) for Eq. (2) we finally obtain

$$\partial_{ZZ}\varphi-(\partial_{XX}+\partial_{YY})\varphi-\eta\varphi+G\varphi^3=0, \tag{4}$$

where $\eta=EV/g$, $G=V/\kappa^2\kappa_z$. Polariton WF φ obviously obeys a normalization condition

$$\int_0^L dX\int_0^L dY\int_0^{L_Z}\varphi^2 dZ|_{t=0}\simeq N_{\rm in}, \tag{5}$$

where $N_{\rm in}$ is the initial total number of polaritons, the dimensionless variables $X=p(t)x/\kappa$, $Y=p(t)y/\kappa$, $Z=p(t)z/\kappa_z$; $\bar{t}=p(t)t$; $L_X=L_Y=L$ and L_Z are characteristic dimensionless lengths of the structure.

Linear regime.—The most interesting features of Eq. (4) can be elucidated in the linear regime, i.e., for the ideal gas of noninteracting polaritons occurring at $g\simeq 0$ and for the vanishing decay rate $\gamma_0\simeq 0$. This approach is equivalent to the low density limit, where nonlinear effects caused by polariton-polariton interactions can be neglected. In this limit, the effective dispersion relation is obtained from Eq. (4) substituting the plane wave solution $\Psi\propto e^{i\mathrm{QR}}$: $\eta=Q_X^2+Q_Y^2-Q_Z^2$. The corresponding dispersion surface is shown in Fig. 2(a). The specific dispersion of Bragg polaritons leads to the characteristic HMM divergence of the photonic density of states [4]. In the same limit, Eq. (4)

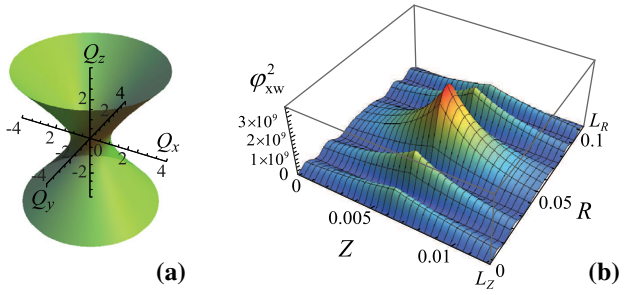

FIG. 2 (color online). (a) Isofrequency surface for Bragg exciton polaritons in the linear dissipationless regime at $g\simeq 0$, $\gamma_0\simeq 0$. Values of $Q_{X,Y,Z}$ are given in $\sqrt{\eta}$ units. The effective masses of polaritons in the structure are $m_\parallel\approx 5.6\times10^{-35}$ kg, $m_\perp\approx -0.8\times10^{-36}$ kg. (b) Normalized probability density φ^2_{xw} vs spatial R and Z variables; $(R-R_0)^2=(X-X_0)^2+(Y-Y_0)^2$. The parameters are: $\Delta=0.031$, $Z_0=L_Z/2$, $R_0=L_R/2=L/\sqrt{2}$, $L_Z\approx 0.012$, $L\approx 0.076$, $\eta\approx 4.45\times10^4$, $N_{\rm in}\approx 3.43\times10^4$. Values of the parameters (except Δ) are taken the same as for Fig. 3 and are discussed below.

supports the so-called X-wave solution defined as $\varphi_{xw}=\mathbb{C}\mathrm{Re}[v^{-1/2}\exp(-i\sqrt{v})]$ (cf. [27]), where we have redefined $v=\eta\{[\Delta-i(Z-Z_0)]^2+(X-X_0)^2+(Y-Y_0)^2\}$; Δ is a real-valued arbitrary coefficient that determines the wave packet localization, X_0, Y_0, and Z_0 define positions of the center of the wave packet, $\mathbb{C}$ is the normalization constant which can be estimated using the normalization condition, Eq. (5). The solution φ^2_{xw} is shown in Fig. 2(b) for the parameters given above. Physically, the polaritonic X wave represents a nondiffracted localized wave packet analogous to diffractionless beams in optics [28].

Polariton Higgs field.—The behavior of our polariton system is essentially modified in the presence of polariton-polariton scattering, i.e., at $g\neq 0$. Equation (4) with the "time" variable Z represents the Ginzburg-Landau-Higgs (GLH) equation, that is typically discussed in connection with the Universe properties and bubble evolution [29]. In order to study Eq. (4) it is convenient to represent the Higgs field φ as a complex scalar field $\varphi=\varphi_1+i\varphi_2$. The "Mexican hat" Higgs potential $W\equiv W(\varphi_1,\varphi_2)$ is shown in Fig. 3(a). The false vacuum state corresponds to $\varphi=0$ while two real vacuum states are located at $\varphi_\pm=\pm\sqrt{\eta/G}\equiv\pm s$ [11]. These two states correspond to two minima of Higgs field potential. The state $\varphi=0$ is unstable vs fluctuations, while the states $\varphi_\pm$ are stable. The behavior of a polariton system governed by Eq. (4) can be easily understood if we consider small perturbations $\tilde{\varphi}_{1,2}$ defined by $\varphi_1=\varphi_0+\tilde{\varphi}_1$, $\varphi_2=\tilde{\varphi}_2$ $(\tilde{\varphi}_{1,2}\ll\varphi_0)$ where φ_0 is the ground state solution of Eq. (4).

Taking into account the global $U(1)$ symmetry properties of the Lagrangian for Eq. (4) it is possible to conclude that the field $\tilde{\varphi}_1$ possesses a mass whereas the field $\tilde{\varphi}_2$ is massless and represents a Nambu-Goldstone boson. Here we focus on φ_1 field properties. In order, Eq. (4) supports a classical (static) kink or black soliton solution

$$\varphi_0(X,Y)=\pm s\tanh[\Theta], \tag{6}$$

where $\Theta\equiv\sqrt{\eta}(X-X_0+Y-Y_0)/2$. In Eq. (6) the parameters X_0, Y_0 characterize the position of the envelope minimum. At $X,Y\to\infty$ the soliton solution in Eq. (6) approaches two vacuum states $\varphi_\pm$. Combining Eqs. (5) and (6) we obtain a condition: $N_{\rm in}\simeq L_Z(L^2\eta-8\ln\{\cosh[\tilde{L}]\})/G$, that determines the critical number of particles required for a kink formation. Here we assume that $X_0=Y_0=L/2$ and introduce the dimensionless parameter $\tilde{L}=L\sqrt{\eta}/2$.

The parameter $s=\sqrt{\eta/G}$ in Eq. (6) plays a crucial role in the field theory, see, e.g., Ref. [11]. In the limit $s\gg 1$, the soliton can be treated as a classical object. We consider

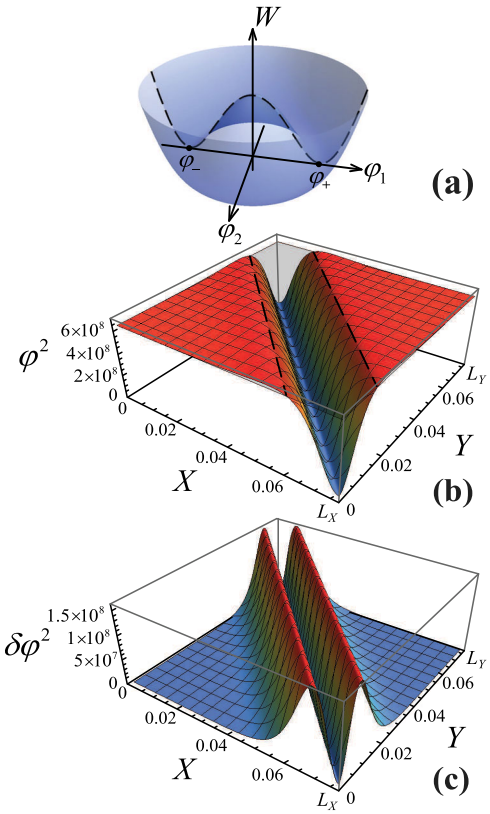

FIG. 3 (color online). (a) Schematic of Higgs potential W versus φ_1 and φ_2 variables, (b) perturbed Higgs field (black soliton) φ^2, and (c) perturbation $\delta\varphi^2$ versus dimensionless spatial coordinates X and Y. The parameters are $X_0 = Y_0 = L/2$, $Z = Z_0 = \pi/2\tilde{\Omega}$, $\mu = 0.2$, $L_x = L_y = 1.5$ μm, $L_z = 2$ μm, $g/V = 1.58$ μeV, $E_1 = 70$ meV. Upper shadow plane $\phi^2 = \eta/G$ in (b) indicates vacuum state solution.

the oscillon field as a small perturbation for the φ function in Z direction. In order to find it, we represent φ in the form $\varphi = \varphi_0 + \mu\delta\varphi$ ($\tilde{\varphi}_1 \equiv \mu\delta\varphi$), where the oscillon solution $\delta\varphi = \delta\varphi(X, Y)\cos(\tilde{\Omega}(Z - Z_0))$ characterizes lateral excitations; we assume that the condition $|\varphi_0| \gg \mu|\delta\varphi|$ is fulfilled. Substituting φ and Eq. (6) in Eq. (4) and linearizing it with respect to $\delta\varphi$, we obtain a Schrödinger-like equation $\hat{F}\delta\varphi(X, Y) = \tilde{\Omega}^2\delta\varphi(X, Y)$ for eigenstates ($\delta\varphi$) and eigenvalues ($\tilde{\Omega}$) of the operator $\hat{F} = -\nabla_\parallel^2 + 2\eta - 3\eta\,\mathrm{sech}^2[\Theta]$. For $\tilde{\Omega}^2 = 3\eta/2$ the first excited state of the system is given by $\delta\varphi(X, Y) = s\tanh[\Theta]\mathrm{sech}[\Theta]$.

The classical kink state φ_0 becomes perturbed due to low amplitude oscillations (fluctuations) of the Higgs field φ, the state being called "Higgs oscillon".

In Fig. 3(b) the perturbed kink φ^2 as a function of X and Y at fixed "time" coordinate Z is plotted. At $X \to \infty$ and $Y \to \infty$ the black soliton solution approaches two vacuum states $\varphi_\pm^2$ as the shadow plane in Fig. 3(b) shows. Taking into account the finite size of the lattice in X and Y directions and the periodicity of the system in the Z direction (with a period of $2\pi/\tilde{\Omega}$) we consider the oscillon formation in a 3D box $L_X \times L_Y \times L_Z$. We write down the condition $\eta = 2\pi^2 n^2/3L_Z^2$, which is relevant to the normalized energy $\eta \equiv E_n V/g$. The square of a quantized Higgs oscillon amplitude $\delta\varphi^2$ is plotted in Fig. 3(c) for the ground state ($n = 1$).

Let us note that the energy density J of the polariton Higgs field is $J = \frac{1}{2}[(\partial_Z\varphi)^2 + (\partial_X\varphi)^2 + (\partial_Y\varphi)^2 - \eta\varphi^2 + (G/2)\varphi^4]$, while the energy density J_0 of the kink is $J_0 = \frac{1}{2}[(\partial_X\varphi_0)^2 + (\partial_Y\varphi_0)^2 - \eta\varphi_0^2 + (G/2)\varphi_0^4]$. Since $|\varphi_0| \gg \mu|\delta\varphi|$, J approaches J_0. Integrating J_0 over the space coordinates X, Y we obtain the energy density in the Z direction as

$$E_{0,Z} = \frac{\eta}{3G}(2 - 3\tilde{L}^2 + 8\ln[\cosh[\tilde{L}]] - 2\mathrm{sech}^2[\tilde{L}]). \quad (7)$$

The energy density of "vacuum" states $\varphi_\pm$ is $J_\pm = \frac{1}{2}[-\eta\varphi_\pm^2 + (G/2)\varphi_\pm^4]$. Hence the energy density in the Z direction is $E_{\pm,Z} = -\tilde{L}^2\eta/G$. Taking into account Eq. (7) one can introduce the effective mass of the kink $M \sim E_{0,Z} - E_{\pm,Z}$. Physically static dark soliton behaves as a relativistic particle with energy $E = Mc^2$ at rest, where c is the speed of light, cf. [29]. Note that M is dependent on the size of the lattice structure.

Topological Schrödinger cat states.—Now let us discuss the Higgs field properties beyond the mean field theory. The quantum tunneling between states $\varphi_\pm$ representing two minima of the Higgs potential, Fig. 3(a) is responsible for creation of field bubbles in the gauge field theory [11]. The tunneling leads to formation of the superposition (Schrödinger cat) states $|\psi_\pm\rangle = [1/\sqrt{2(1 + e^{-2s^2})}](|\phi_+\rangle \pm |\phi_-\rangle)$, where $|\phi_+\rangle$ and $|\phi_-\rangle$ are macroscopically distinguishable Glauber's coherent states associated with fields ϕ_+ and ϕ_-, respectively. The "size of the cat" can be estimated via the overlap integral of the states $|\phi_\pm\rangle$ as $\zeta = 1/\langle\phi_+|\phi_-\rangle = e^{2s^2}$ [30]. The parameter ζ becomes larger in the limit $s \gg 1$ which is indeed experimentally achievable in realistic structures [Eq. (6)]. Notably, the properties of states $|\psi_\pm\rangle$ are highly nonclassical, see e.g., Ref. [31]. In particular, due to the interference, a fringe pattern occurs between Gaussian bells representing states $|\phi_\pm\rangle$ in the Wigner function approach. The negativity of this function that is inherent to the states $|\psi_\pm\rangle$ is responsible for that. While the states $|\psi_\pm\rangle$ involve a macroscopically large number of particles they can be used for the generation of macroscopic entangled states (cf. [32]) of exciton polaritons in Bragg superlattices. The computational qubit states $|0\rangle$ and $|1\rangle$ can be associated with mutually orthogonal states as $|0\rangle = |\psi_+\rangle$ and $|1\rangle = |\psi_-\rangle$, cf. Ref. [33]. Alternatively, if the parameter e^{-2s^2} vanishes rapidly, the topological states $|\phi_+\rangle$ and $|\phi_-\rangle$ for the quantum Higgs field itself may be considered as computational qubit states $|0\rangle$ and $|1\rangle$ [34]. In this case qubit operations presume implementation of linear circuit

networks and conditional photon detection [35]. Fortunately, such circuits can be designed using well developed semiconductor technologies, [36,37].

In conclusion, we propose the realization of quantum HMMs in a periodic planar semiconductor Bragg mirror with embedded QWs. We demonstrate mapping of the polaritonic GPE onto a nonlinear GLH equation, which exhibits physically nontrivial features. In the linear case, i.e., for noninteracting LB polaritons, we obtain a polariton X-wave solution that is reminiscent of a nondiffractive (spatially localized) matter wave packet. We predict formation of kink-shaped states for weakly interacting polaritons. Small amplitude oscillations (oscillons) occur in a perturbed polariton Higgs field due to fluctuations. Going beyond the mean field theory, we obtain a Schrödinger cat state as a macroscopic superposition of two vacuum states $\varphi_{\pm}$. Polaritonic nonlinear HMMs have a high potentiality for the simulation of fundamental cosmological processes. We are confident that the dissipative nature of exciton polaritons should not be a major obstacle for observation of the proposed coherent phenomena in state-of-the-art semiconductor Bragg structures. We note that due to the short polariton lifetime, the coherent effects discussed in this Letter are transient in a sense. In particular, the coherent dynamics of polariton liquids may be accessed by coherent methods of time-resolved spectroscopy, e.g., pump-probe spectroscopy.

This work was supported by Russian Foundation for Basic Research Grants No. 14-02-31443, No. 14-02-92604, No. 14-32-50420, No. 14-02-97503, No. 15-52-52001, No. 15-59-30406, by the Russian Ministry of Education and Science state tasks No. 2014/13, 16.440.2014/K, 3.1231.2014/K, by President grants for leader scientific schools No. 89.2014.2, MK-5220.2015.2 and European Union project PIRSES-GA-2013-612600 LIMACONA. A. P. A. acknowledges support from "Dynasty" Foundation.

*evgeny_sedov@mail.ru
†alodjants@vlsu.ru

[1] H. Chen, C. Chan, and P. Sheng, Nat. Mater. **9**, 387 (2010).
[2] C. Sheng, H. Liu, Y. Wang, S. N. Zhu, and D. A. Genov, Nat. Photonics **7**, 902 (2013).
[3] U. Leonhardt and T. Philbin, Prog. Opt. **53**, 69 (2009).
[4] M. McCall, Contemp. Phys. **54**, 273 (2013).
[5] J. B. Pendry, Phys. Rev. Lett. **85**, 3966 (2000).
[6] J. B. Pendry, A. J. Holden, D. J. Robbins, and W. J. Stewart, IEEE Trans. Microwave Theory Tech. **47**, 2075 (1999).
[7] A. Poddubny, I. Iorsh, P. A. Belov, and Yu. S. Kivshar, Nat. Photonics **7**, 948 (2013).
[8] Z. Jacob, J.-Y. Kim, G. V. Naik, A. Boltasseva, E. E. Narimanov, and V. M. Shalaev, Appl. Phys. B **100**, 215 (2010).
[9] Z. Liu, H. Lee, Y. Xiong, C. Sun, and Z. Zhang, Science **315**, 1686 (2007).
[10] I. I. Smolyaninov, Phys. Rev. A **88**, 033843 (2013).
[11] V. A. Rubakov, *Classical Theory of Gauge Fields* (Princeton University Press, Princeton, NJ, 2002).
[12] M. V. Charukhchyan, E. S. Sedov, S. M. Arakelian, and A. P. Alodjants, Phys. Rev. A **89**, 063624 (2014).
[13] A. V. Poshakinskiy, A. N. Poddubny, L. Pilozzi, and E. L. Ivchenko, Phys. Rev. Lett. **112**, 107403 (2014).
[14] M. Wouters and I. Carusotto, Phys. Rev. Lett. **99**, 140402 (2007).
[15] M. Abbarchi *et al.*, Nat. Phys. **9**, 275 (2013).
[16] A. Amo *et al.*, Science, **332**, 1167 (2011).
[17] E. L. Ivchenko, S. Jorda, and A. I. Nesvizhskii, Fiz. Tverd. Tela **36**, 2118 (1994) [Phys. Solid State **36**, 1156 (1994)].
[18] A. V. Kavokin and M. A. Kaliteevski, J. Appl. Phys. **79**, 595 (1996).
[19] A. Yu. Sivachenko, M. E. Raikh, and Z. V. Vardeny, Phys. Rev. A **64**, 013809 (2001).
[20] F. Biancalana, L. Mouchliadis, C. Creatore, S. Osborne, and W. Langbein, Phys. Rev. B **80**, 121306(R) (2009); C. Creatore, L. Mouchliadis, F. Biancalana, S. Osborne, and W. Langbein, J. Phys. Conf. Ser. **210**, 012034 (2010).
[21] A. Kavokin, J. J. Baumberg, G. Malpuech, and F. P. Laussy, *Microcavities* (Oxford University Press, New York, 2007).
[22] A. Askitopoulos, L. Mouchliadis, I. Iorsh, G. Christmann, J. J. Baumberg, M. A. Kaliteevski, Z. Hatzopoulos, and P. G. Savvidis, Phys. Rev. Lett. **106**, 076401 (2011).
[23] See Supplemental Material at http://link.aps.org/supplemental/10.1103/PhysRevLett.114.237402 for the methods used to obtain dependencies in Fig. 1 and the Gross-Pitaevskii equation for Bragg exciton polaritons, which includes Refs. [24,25].
[24] L. M. Brekhovskikh, *Waves in Layered Media* (Academic, New York, 1980).
[25] F. Dalfovo, S. Giorgini, L. P. Pitaevskii, and S. Stringari, Rev. Mod. Phys. **71**, 463 (1999).
[26] M. Onorato and D. Proment, Phys. Lett. A **376**, 3057 (2012).
[27] C. Conti, S. Trillo, P. Di Trapani, G. Valiulis, A. Piskarskas, O. Jedrkiewicz, and J. Trull, Phys. Rev. Lett. **90**, 170406 (2003); C. Conti, Phys. Rev. E **68**, 016606 (2003).
[28] J. Durnin, J. J. Miceli, and J. H. Eberly, Phys. Rev. Lett. **58**, 1499 (1987).
[29] V. G. Makhankov, Phys. Rep. C **35**, 1 (1978).
[30] J. I. Cirac, M. Lewenstein, K. Molmer, and P. Zoller, Phys. Rev. A **57**, 1208 (1998).
[31] B. Yurke and D. Stoler, Phys. Rev. Lett. **57**, 13 (1986).
[32] B. C. Sanders, Phys. Rev. A **45**, 6811 (1992).
[33] M. C. de Oliveira and W. J. Munro, Phys. Rev. A **61**, 042309 (2000).
[34] T. C. Ralph, A. Gilchrist, G. J. Milburn, W. J. Munro, and S. Glancy, Phys. Rev. A **68**, 042319 (2003).
[35] E. Knill, R. Lafamme, and G. J. Milburn, Nature (London) **409**, 46 (2001).
[36] D. Ballarini, M. De Giorgi, E. Cancellieri, R. Houdré, E. Giacobino, R. Cingolani, A. Bramati, G. Gigli, and D. Sanvitto, Nat. Commun. **4**, 1778 (2013); M. De Giorgi *et al.*, Phys. Rev. Lett. **109**, 266407 (2012).
[37] S. S. Demirchyan, I. Yu. Chestnov, A. P. Alodjants, M. M. Glazov, and A. V. Kavokin, Phys. Rev. Lett. **112**, 196403 (2014).